Heisenberg-Limited Noisy Atomic Clock Using a Hybrid Coherent and Squeezed State Protocol

Luca Pezzè and Augusto Smerzi
QSTAR, INO-CNR and LENS, Largo Enrico Fermi 2, 50125 Firenze, Italy

(Received 26 March 2020; accepted 29 September 2020; published 19 November 2020)

We propose a hybrid quantum-classical atomic clock where the interrogation of atoms prepared in a spin-coherent (or weakly squeezed) state is used to feed back one or more highly spin-squeezed atomic states toward their optimal phase-sensitivity point. The hybrid clock overcomes the stability of a single Ramsey clock using coherent or optimal spin-squeezed states and reaches a Heisenberg-limited stability while avoiding nondestructive measurements. When optimized with respect to the total number of particles, the protocol surpasses the state-of-the-art proposals that use Greenberger-Horne-Zeilinger or NOON states. We compare analytical predictions with numerical simulations of clock operations, including correlated $1/f$ local oscillator noise.

DOI: 10.1103/PhysRevLett.125.210503

Atomic clocks provide stable and accurate frequency and time references [1,2]. These are crucial for technological applications and fundamental research—from relativistic geodesy [3–6] to the search for variations of the fine-structure constant [7–9]. Intense efforts are currently focusing on new strategies to further increase the stability of atomic clocks. These include the realization of low-decoherence lasers [10,11], the decrease of interrogation dead times [12–14], and the reduction of phase estimation uncertainties below the standard quantum limit (SQL) $\Delta\theta_{\mathrm{SQL}} = 1/\sqrt{N}$ [15,16], a bound imposed by quantum mechanics when using N classically correlated atoms [17–19]. In principle, the clock sensitivity can arbitrarily increase with the number of atoms. In realistic scenarios, however, N is limited either by the use of specific non-scalable platforms or by decoherence effects like collisional shifts and three-body recombinations. The possibility of overcoming the SQL by creating tailored quantum correlations among the atoms is therefore attracting increasing interest [15]. Experiments have explored the creation of spin-squeezed states [20–25] with Bose–Einstein condensates [26–28], trapped ions [29], and cold atoms [30–33], demonstrating proof-of-principle atom interferometers with sensitivities overcoming the SQL [15,16,33–36]. Squeezed states have reduced fluctuations of some chosen observable with respect to spin-coherent states and are far more robust to decoherence than Greenberger-Horne-Zeilinger (GHZ) or NOON states. Squeezed states are therefore good candidates for magnetometers [37–39] and atom interferometers [40] with performances overcoming the current technology. However, the possible advantages offered by squeezing in noisy atomic clocks, where the main sources of noise are the fluctuations of the local oscillator (LO) during a Ramsey interrogation, is still debated [41–47]. The reason is that squeezed states allow one to decrease the phase uncertainty $\Delta\theta$ below the SQL only when the unknown phase θ is sufficiently close to the optimal point θ_{opt} of the Ramsey interference fringes, while $\Delta\theta$ rapidly degrades once θ drifts away. In addition, the more the state is squeezed, the narrower is the range of phase values where $\Delta\theta < \Delta\theta_{\mathrm{SQL}}$. These effects dramatically limit the usefulness of squeezed states to increase the long-term stability of noisy clocks, providing an Allan variance $\sigma^2_{\mathrm{sq}} \sim N^{-4/3}$ [41] far from the Heisenberg scaling $\sigma^2_{\mathrm{HL}} \sim N^{-2}$. The possibility of overcoming this limitation has triggered many efforts to develop protocols combining squeezing and nondestructive measurements [42,43]. Unfortunately, back-action effects introduce a loss of atomic coherence [48–50] that limits the performances of these protocols.

Here we propose an atomic clock where a single coherent and a few spin-squeezed states interrogate the same LO. Figure 1 illustrates a hybrid coherent-squeezed clock using two states. The central idea is to take advantage of the θ-independent sensitivity of the coherent state to steer, via a phase feedback, the squeezed state toward its optimal sensitivity point (namely toward the equatorial plane of the Bloch sphere in Fig. 1). In practice, to increase the stability, it is desirable to run each interferometer with the maximum number of particles, N, available. The clock, using $\nu \geq 2$ optimized states with the same number of particles, N, (a coherent state and $\nu - 1$ spin-squeezed states), reaches an Allan variance $\sigma^2_{\nu,\mathrm{opt}} \sim N^{-2+1/3^{\nu-1}}$, which asymptotically saturates the Heisenberg scaling. An even higher stability is obtained for the cascade joint interrogation of ν optimal spin-squeezed states. When optimizing over the number of ensembles for a fixed total number of particles, $N_t = \nu N$, the stability of the hybrid atomic clock surpasses the best proposal discussed so far in the

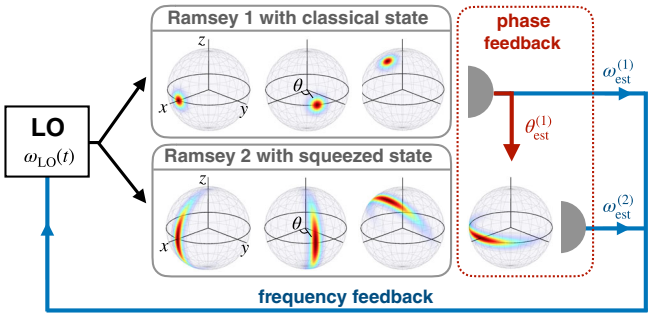

FIG. 1. Hybrid scheme with two atomic clocks interrogating the same local oscillator. Both Ramsey interferometers consist of state preparation (left-hand side showing the Husimi distribution), phase shift (center—the interrogation time T, and thus the accumulated phase θ, is the same for both ensembles), and $\pi/2$ rotation about the x axis (right). Ramsey 1 uses a coherent spin state, while Ramsey 2 uses a spin-squeezed state. Before readout, Ramsey 2 is rotated around the y axis by the angle $\theta_{\rm est}^{(1)}$ obtained from the phase estimate in Ramsey 1. This implements a phase feedback (red line) that places the spin-squeezed state of Ramsey 2 close to its most sensitive phase estimation point. The frequency estimates $\omega_{\rm est}^{(1,2)} = \theta_{\rm est}^{(1,2)}/T$ are combined to steer (blue lines) the frequency of the local oscillator by $\omega_{\rm est}^{(1)} + \omega_{\rm est}^{(2)}$.

literature [44] that uses GHZ or NOON states and achieves $\sigma_{\rm GHZ}^2 \sim \log N_t/N_t^2$. The high stability of our clock is reached using robust states that are now routinely created in labs with large numbers of atoms and without requiring entanglement between different atomic ensembles or the implementation of nondestructive measurements.

Stability of a hybrid coherent-squeezed clock.—A passive atomic clock operates by locking, via a feedback loop, the frequency of a laser to the energy transition of a two-level atom [51]. In the hybrid clock illustrated in Fig. 1, a Ramsey interferometric sequence is identically applied to a coherent spin state made by uncorrelated atoms and to a spin-squeezed state. A free precession about the z axis of the Bloch sphere rotates the atomic states by the same angle $\theta = \int_T dt \delta\omega_{\rm LO}(t)$ during the interrogation time T (which is the same in both states), where $\delta\omega_{\rm LO}(t) = \omega_{\rm LO}(t) - \omega_0$, $\omega_{\rm LO}(t)$ is the time-dependent locked LO frequency and ω_0 is the reference atomic frequency. After having accumulated the same phase, both states are rotated around the x axis by an angle $\pi/2$.

The central operation of the hybrid clock is the phase feedback (see Fig. 1). First, the relative population difference $\hat{J}_z$ between the two atomic hyperfine levels in the Ramsey interferometer using the coherent state is measured [52]. Given the result $-N/2 \le \mu \le N/2$, the phase is estimated as $\theta_{\rm est}^{(1)} = \arcsin(2\mu/N)$, with a sensitivity $\Delta\theta_{\rm est}^{(1)} = 1/\sqrt{N}$, independently of θ [53]. The phase feedback is implemented by a rotation of the spin-squeezed state by the angle $\theta_{\rm est}^{(1)}$ about the y axis. The spin-squeezed state is thus rotated toward the equatorial plane of the Bloch sphere within an uncertainty region of the order of $1/\sqrt{N}$ about its most sensitive phase estimation point $\theta_{\rm opt} = 0$. This is the key idea of this proposal. The overall transformation of the spin-squeezed state is equivalent to a Ramsey sequence with an accumulated phase equal to $\theta - \theta_{\rm est}^{(1)}$ (see Fig. 1). The measurement of the relative number of particles provides an estimate $\theta_{\rm est}^{(2)}$ of $\theta - \theta_{\rm est}^{(1)}$. We emphasize here that $\theta_{\rm est}^{(1)}$ plays the role of a stochastic but exactly determined number that has to be added to the unknown stochastic value θ that we want to estimate. In other words, the estimation uncertainty of $\theta_{\rm est}^{(1)}$ does not propagate to the error of the final estimation. Therefore, $\theta_{\rm est} = \theta_{\rm est}^{(1)} + \theta_{\rm est}^{(2)}$ estimates θ with a sensitivity $(\Delta\theta_{\rm est})^2 = [\Delta\theta_{\rm est}^{(2)}]^2$. Finally, the LO frequency is steered by $\omega_{\rm est} = \theta_{\rm est}/T$.

In the following, we consider the unlocked LO $\tilde{\omega}_{\rm LO}(t)$ with power spectrum $S(f) = 2\gamma_{\rm LO}^2/f$ [51], where $\delta\tilde{\omega}_{\rm LO}(t) = \tilde{\omega}_{\rm LO}(t) - \omega_0$ has a time-independent variance $\mathcal{E}[\delta\tilde{\omega}_{\rm LO}(t)^2] = \gamma_{\rm LO}^2$ and zero mean $\mathcal{E}[\delta\tilde{\omega}_{\rm LO}(t)] = 0$, and $\mathcal{E}$ indicates statistical averaging. These fluctuations are a most important source of noise in realistic clocks, where atomic decoherence typically occurs on longer time scales. Our analysis also neglects the effect of dead times [47] and dephasing during clock operations. We quantify the stability of the clock by

$$\sigma^2 = \frac{\mathcal{E}[(\Delta\theta_{\rm est})^2]}{\omega_0^2 \tau T}, \tag{1}$$

where τ is the total averaging time and $\Delta\theta_{\rm est} = \theta - \theta_{\rm est}$ is the difference between the phase shift and its estimated value. We show in the Supplemental Material [53] that Eq. (1) corresponds to the Allan variance (see also [41–44]). In the following, we derive a simple analytical approximation of Eq. (1) and compare it to numerical simulations of the full clock operations.

We recall here that $(\Delta\theta_{\rm est})^2 = [\Delta\theta_{\rm est}^{(2)}]^2$ and the statistical averaging in Eq. (1) can be evaluated as $\mathcal{E}\{[\Delta\theta_{\rm est}^{(2)}]^2\} = \int d\phi P(\theta_2)[\Delta\theta_{\rm est}^{(2)}]^2$, where $[\Delta\theta_{\rm est}^{(2)}]^2 = \sum_\mu [\theta_{\rm est}(\mu) - \theta_2]^2 P(\mu|\theta_2)$ is the estimator variance, $P(\mu|\theta_2)$ is the conditional probability to obtain the measurement result μ for a given stochastic $\theta_2 = \theta - \theta_{\rm est}^{(1)}$ with distribution $P(\theta_2)$. In the following, we take $P(\theta_2) \sim e^{-\theta_2^2/(2\kappa_1^2)}$, where the width κ_1 quantifies the phase noise of θ_2. From error propagation we have

$$[\Delta\theta_{\rm est}^{(2)}]^2 = \frac{(\Delta\hat{J}_y)^2}{\langle\hat{J}_x\rangle^2} + \frac{(\Delta\hat{J}_x)^2}{\langle\hat{J}_x\rangle^2}\theta_2^2, \tag{2}$$

where the spin moments on the r.h.s of Eq. (2) are calculated for the input state of the second interferometer $|\psi_2\rangle$ [53]. Analytical results can be obtained with $|\psi_2\rangle \sim \int d\mu\, e^{-\mu^2/(s_2^2 N)}|\mu\rangle_y$, where s is a squeezing parameter ($s < 1$ for metrological spin-squeezed states

[15,21,23]) and $|\mu\rangle_y$ are eigenstates of $\hat{J}_y$. We get $(\Delta\hat{J}_y)^2 = s_2^2 N/4$, $\langle \hat{J}_x \rangle = (N/2)e^{-1/(2s_2^2 N)}$, and $\langle \hat{J}_x^2 \rangle = (N^2/8)[1 + e^{-2/(s_2^2 N)}]$ [53]. Replacing into Eqs. (1) and (2), for $s_2^2 N \gg 1$, we obtain

$$\sigma_2^2 = \frac{1}{\omega_0^2 \tau T}\left(\frac{s_2^2}{N} + \frac{\kappa_1^2}{2 s_2^4 N^2}\right). \tag{3}$$

In the absence of fringe hops, namely when $|\theta| \lesssim \pi/2$, the fluctuations of θ_2 are dominated by the quantum phase noise due to the phase estimation in the first interferometer, namely $\kappa_1^2 = 1/N$. Replacing this value into Eq. (3) and optimizing over the squeezing parameter gives $s_{2,\mathrm{opt}}^2 = N^{-2/3}$ [53], verifying the assumption $s_{2,\mathrm{opt}}^2 N = N^{1/3} \gg 1$ for $N \gg 1$, and finally

$$\sigma_{2,\mathrm{opt}}^2 = \frac{1}{\omega_0^2 \tau T} \times \frac{3}{2}\frac{1}{N^{5/3}}. \tag{4}$$

This is the most important result of this paper for the hybrid clock of Fig. 1, which is based on the interrogation of two atomic states. This result will be extended in the next sections.

Equation (4) shows a scaling of the stability with respect to the number of atoms N that is superior to the one reached by optimal spin-squeezed states in a single Ramsey clock, $\sigma_{\mathrm{sq}}^2 \sim N^{-4/3}$ [41]. It is worthwhile to briefly elaborate on this point. For large squeezing, the second term in r.h.s. of Eq. (3) becomes significant due to the bending of the state in the equatorial plane of the Bloch sphere and strongly depletes the sensitivity except in a restricted phase interval around $\theta_{\mathrm{opt}} = 0$ where can we still expect sub-SQL sensitivities. High sensitive atomic clocks work in regimes of large Ramsey times, which means large (stochastic) phase shifts $|\theta| \lesssim \pi/2$. Therefore, a single Ramsey clock operating with a spin-squeezed state would mostly explore suboptimal phase sensitivity regions, eventually providing only modest improvements with respect to the SQL [41]. The sub-SQL region shrinks with s and only a modest spin-squeezing parameter is optimal for the single Ramsey clock. In contrast, the hybrid clock allows the use of states having much higher squeezing ($s_{2,\mathrm{opt}} \ll 1$).

In Fig. 2, we show the stability of the optimized hybrid clock as a function of the interrogation time T, with $N = 10^6$ particles in each state. Equation (4) is in excellent agreement with the numerical results [54] up to $\gamma_{\mathrm{LO}} T \approx 0.4$, where phase slips become likely and deplete the stability. We compare the performance of the hybrid coherent-squeezed clock with that of a single atomic clocks operating with a coherent spin state of $N = 2 \times 10^6$ particles, where the optimal interrogation time is also given by $\gamma_{\mathrm{LO}} T \approx 0.4$. In this case, the clock has an SQL Allan variance [1,17]

$$\sigma_{\mathrm{SQL}}^2 = \frac{1}{\omega_0^2 \tau T N}. \tag{5}$$

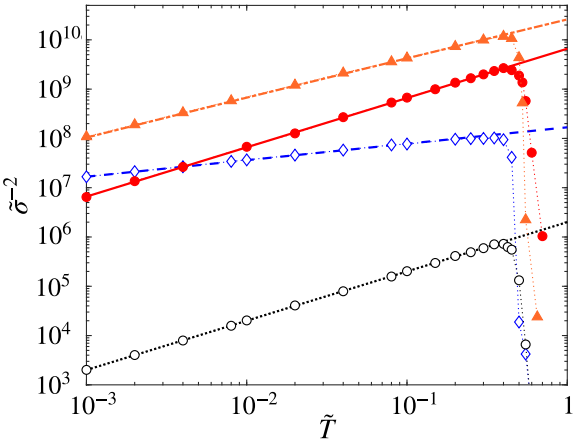

FIG. 2. Inverse Allan variance as a function of the interrogation time T for the hybrid clock implemented with two ensembles of $N = 10^6$ particles each: (i) a coherent state and an optimal squeezed state (red circles), the solid red line being Eq. (4), and (ii) optimal spin-squeezed states (orange triangles) with the dot-dashed orange line being Eq. (10) with $\nu = 2$. For comparison, we show the inverse Allan variance for a Ramsey clock using a coherent spin state (black circles) and an optimal spin-squeezed state (blue diamonds) of $N = 2 \times 10^6$ particles. The black dotted line is σ_{SQL}^2, Eq. (5), while the blue dashed line is σ_{sq}^2, Eq. (6). Here we have used rescaled units $\tilde{T} = \gamma_{\mathrm{LO}} T$, $\tilde{\sigma} = \sigma\omega_0\sqrt{\tau/\gamma_{\mathrm{LO}}}$. The thin dotted lines are guides to the eye.

The hybrid clock surpasses by orders of magnitude the SQL long-term stability. It also overcomes the long-term stability reached by a single clock operating with a spin-squeezed state of $N = 2 \times 10^6$ particles with the squeezing parameter optimized for each Ramsey time T. The corresponding Allan variance

$$\sigma_{\mathrm{sq}}^2 = \frac{3}{2}\frac{1}{\omega_0^2 \tau}\left(\frac{\gamma_{\mathrm{LO}}^2}{T N^4}\right)^{1/3} \tag{6}$$

is obtained for an optimal squeezing parameter $s_{\mathrm{sq}}^2 = (\gamma_{\mathrm{LO}}^2 T^2/N)^{1/3}$. The hybrid clock using $2N$ atoms in total leads to a smaller Allan variance than the Ramsey clock using a single optimal squeezed state of $2N$ atoms for an interrogation time $\gamma_{\mathrm{LO}} T \geq 4/\sqrt{N}$, which is obtained by comparing Eq. (4) to σ_{sq}^2.

Extended coherent-squeezed clock.—We now extend the hybrid clock discussed above by considering three or more atomic states having the same number of atoms, N, and interrogating the same LO. In this case, the phase feedback is implemented by rotating the state of the third Ramsey interferometer by $\theta_{\mathrm{est}}^{(1)} + \theta_{\mathrm{est}}^{(2)}$ around the y axis before readout, where $\theta_{\mathrm{est}}^{(2)}$ is the estimated phase from the second Ramsey interferometer, and so on. In a cascade of ν states (one coherent and $\nu - 1$ spin-squeezed) [53] the optimal value of the squeezing for the νth state is

$$s^2_{\nu,\mathrm{opt}} = \left(\frac{3}{2}\right)^{\frac{1}{2}[1-(1/3^{\nu-2})]} \frac{1}{N^{1-1/3^{\nu-1}}}, \tag{7}$$

which provides the optimized Allan variance

$$\sigma^2_{\nu,\mathrm{opt}} = \frac{1}{\omega_0^2 \tau T} \times \left(\frac{3}{2}\right)^{\frac{3}{2}[1-(1/3^{\nu-1})]} \frac{1}{N^{2-1/3^{\nu-1}}}. \tag{8}$$

These equations assume $s^2_{\nu,\mathrm{opt}} N \sim N^{1/3^{\nu-1}} \gg 1$, which require asymptotically large N [53]. Equation (8) quickly approaches $\sigma^2_{\nu,\mathrm{opt}} \sim 1/(\omega_0^2 \tau T N^2)$ when $3^{\nu-1} \gg 1$ with a prefactor $(3/2)^{3/2} \approx 1.84$. This is the second main result of this paper, which extends Eq. (4) to the case of more than two atomic states. By increasing ν, optimal states are more and more squeezed [Eq. (7)], which provides an increase in long-term stability compared to Eq. (6).

In Fig. 3(a), we show the scaling with N of the optimized Allan variance of the hybrid clock at $\gamma_{\mathrm{LO}} T = 0.1$. The lines are the results of a numerical optimization (see [53]) that agree with Eq. (8) asymptotically in N. All symbols in Fig. 3(a) are the results of Monte Carlo simulations.

Stability of a hybrid squeezed-squeezed clock.—As shown in Fig. 2, for very short interrogation times, the stability of the hybrid coherent-squeezed clock is surpassed by the single Ramsey clock using optimal squeezed states. We thus study here a hybrid scheme where the first interferometer has a spin-squeezed input state rather than a coherent state as considered above. Using a cascade of ν optimized squeezed states leads to [53]

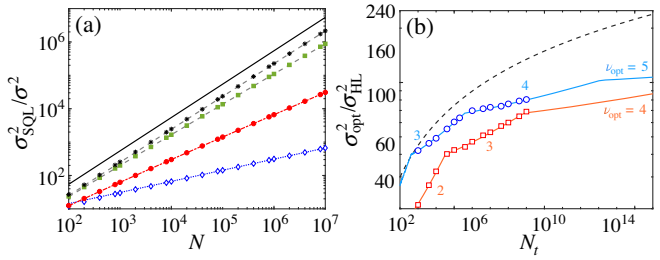

FIG. 3. (a) Rescaled inverse Allan variance as a function of N. The symbols are the numerical results for the single Ramsey clock with optimal squeezed states (blue diamonds) and the hybrid coherent-squeezed clock with $\nu = 2$ (red dots), $\nu = 3$ (green squares), and $\nu = 4$ (black asterisks). The dotted blue line is Eq. (6) for the single Ramsey clock; the dot-dashed red line is Eq. (8) for the hybrid coherent-squeezed clock; the dashed black and green lines are the results of a numerical optimization for the coherent-squeezed clock with $\nu = 3$ and $\nu = 4$, respectively, and agree with Eq. (8) for sufficiently large N. The thick black line is the asymptotic $\nu \to \infty$ prediction of Eq. (8). (b) Allan variance rescaled by $\sigma^2_{\mathrm{HL}} = 1/(\omega^2 T \tau N_t^2)$ as a function of the total number of particles, N_t, for the hybrid clock with ν_{opt} ensembles. The solid blue (red) line is the result of a numerical optimization of the coherent-squeezed (squeezed-squeezed) clock over ν. Circles and squares are results of Monte Carlo simulations for the two protocols, respectively, at $\gamma_{\mathrm{LO}} T = 0.1$. Values of ν_{opt} are indicated in the figure. The black dashed line is σ^2_{GHZ} (see text).

$$s^2_{\nu,\mathrm{opt}} = \left(\frac{3}{2}\right)^{\frac{1}{2}(1-(1/3^{\nu-1})} \frac{(T\gamma_{\mathrm{LO}})^{2/3^{\nu}}}{N^{1-2/3^{\nu}}}, \tag{9}$$

$$\sigma^2_{\nu,\mathrm{opt}} = \frac{1}{\omega_0^2 \tau T} \times \left(\frac{3}{2}\right)^{\frac{3}{2}(1-(1/3^{\nu})} \frac{(T\gamma_{\mathrm{LO}})^{2/3^{\nu}}}{N^{2(1-1/3^{\nu})}}. \tag{10}$$

Equation (6) is recovered for $\nu = 1$. In Fig. 2, we show the numerical results for the stability of the hybrid squeezed-squeezed clock ($\nu = 2$). The hybrid scheme with optimal squeezed states overcomes both the stability of the single squeezed clock and that of the hybrid coherent-squeezed clock (see Fig. 2).

Discussion.—Considering a fixed number of particles, N, in each atomic state is a natural condition in clock experiments, where one increases the stability by interrogating the largest possible number of particles [1]. When fixing the *total* number of particles, N_t, it is possible to optimize the hybrid clock with respect to the number ν of states, defining ν_{opt} (σ^2_{opt} being the corresponding Allan variance), all states having the same $N = N_t/\nu$. Results of this optimization are shown in Fig. 3(b): ν_{opt} increases with N_t, e.g., it is $\nu_{\mathrm{opt}} = 4$ ($\nu_{\mathrm{opt}} = 3$) for the hybrid coherent-squeezed (squeezed-squeezed) clock in the relevant range $10^5 \lesssim N_t \lesssim 10^8$. The scaling of the Allan variance with N_t is arbitrarily close to the Heisenberg scaling for a sufficiently large N_t at the price of an increasing prefactor [53,55]. These results should be compared to the proposal of Ref. [44], which is based on the cascade interrogation of GHZ or NOON states of increasing numbers of particles, and represents the state-of-the-art metrological proposal for timekeeping. Using N_t total particles, optimally distributed in $(16/\pi^2)(\log N_t)^2$ ensembles [44], the GHZ or NOON scheme reaches $\sigma^2_{\mathrm{GHZ}} = (8/\pi)^2 \log(N_t)/(\omega_0^2 T \tau N_t^2)$ [44], shown as the black dashed line in Fig. 3(b). It is remarkable that σ^2_{GHZ} is surpassed in our scheme by using a much smaller number of robust states that are now routinely created in labs. To the contrary, GHZ or NOON states are very fragile to losses and have been created so far up to about $N \approx 20$ particles [56,57].

It is worth noting that the analysis of the hybrid clock can be extended to states that have a fluctuating number of particles, as is common in experiments with cold atoms [15]. As shown in [53], the above results generalize by replacing N with the average number of particles in the state $\bar{N}$. Furthermore, since the readout of the squeezed state ensemble is close to the optimal phase point, we can make use of nonlinear readout schemes to overcome detection noise [58–61]. It is also possible to combine the present hybrid scheme with different protocols proposed in the literature to increase the Ramsey interrogation time [45,62–66] to achieve the optimal condition $T \approx \tau$ [44].

Conclusions.—We have proposed a hybrid clock based on the joint interrogation of a cascade of states of increasingly high spin squeezing and interrogating the same noisy

local oscillator. Despite using spin Gaussian states, the hybrid clock surpasses the state-of-the-art stability reached by GHZ or NOON states [44], while being more resilient to noise and decoherence. The basic principle of our hybrid clock has some analogies with the hybrid quantum computation [67,68] and simulation [69,70] protocols recently explored in the literature, where classical algorithms were combined with quantum resources to speed up specific tasks. Adaptive strategies for measurement optimization—with aims similar to the strategy applied here to frequency stabilization in atomic clocks—are important in quantum state and parameter estimation [71–75].

The clock operations discussed in this Letter, including the creation of atomic spin-squeezed states, measurement, and estimation, are within the current technology.

We acknowledge funding of the project EMPIR-USOQS, EMPIR projects are cofunded by the European Union's Horizon2020 research and innovation program and the EMPIR participating states. We also acknowledge support by the H2020 QuantERA ERA-NET Cofund QCLOCKS.

[1] A. D. Ludlow, M. M. Boyd, J. Ye, E. Peik, and P. O. Schmidt, Optical atomic clocks, Rev. Mod. Phys. **87**, 637 (2015).
[2] N. Poli, C. W. Oates, P. Gill, and G. M. Tino, Optical atomic clocks, Nuovo Cimento **36**, 555 (2013).
[3] C. Lisdat *et al.*, A clock network for geodesy and fundamental science, Nat. Commun. **7**, 12443 (2016).
[4] T. Mehlstaübler, G. Grosche, C. Lisdat, P. O. Schmidt, and H. Denker, Atomic clocks for geodesy, Rep. Prog. Phys. **81**, 064401 (2018).
[5] S. Kolkowitz, I. Pikovski, N. Langellier, M. D. Lukin, R. L. Walsworth, and J. Ye, Gravitational wave detection with optical lattice atomic clocks, Phys. Rev. D **94**, 124043 (2016).
[6] W. F. Mc Grew *et al.*, Atomic clock performance enabling geodesy below the centimetre level, Nature (London) **564**, 87 (2018).
[7] A. Derevianko and M. Pospelov, Hunting for topological dark matter with atomic clocks, Nat. Phys. **10**, 933 (2014).
[8] C. Sanner, N. Huntemann, R. Lange, C. Tamm, E. Peik, M. S. Safronova, and S. G. Porsev, Optical clock comparison for Lorentz symmetry testing, Nature (London) **567**, 204 (2019).
[9] B. M. Roberts *et al.*, Search for transient variations of the fine structure constant and dark matter using fiber-linked optical atomic clocks, New J. Phys. **22**, 093010 (2020).
[10] G. D. Cole, W. Zhang, M. J. Martin, J. Ye, and M. Aspelmeyer, Tenfold reduction of brownian noise in high-reflectivity optical coatings, Nat. Photonics **7**, 644 (2013).
[11] N. Nemitz, T. Ohkubo, M. Takamoto, I. Ushijima, M. Das, N. Ohmae, and H. Katori, Frequency ratio of yb and sr clocks with 5×10^{-17} uncertainty at 150 seconds averaging time, Nat. Photonics **10**, 258 (2016).
[12] M. Takamoto, T. Takano, and H. Katori, Frequency comparison of optical lattice clocks beyond the Dick limit, Nat. Photonics **5**, 288 (2011).
[13] M. Schioppo *et al.*, Ultrastable optical clock with two cold-atom ensembles, Nat. Photonics **11**, 48 (2017).
[14] C. W. Chou, D. B. Hume, M. J. Thorpe, D. J. Wineland, and T. Rosenband, Quantum Coherence between Two Atoms Beyond $q = 10^{15}$, Phys. Rev. Lett. **106**, 160801 (2011).
[15] L. Pezzè, A. Smerzi, M. K. Oberthaler, R. Schmied, and P. Treutlein, Quantum metrology with nonclassical states of atomic ensembles, Rev. Mod. Phys. **90**, 035005 (2018).
[16] E. Pedrozo-Peñfiel, S. Colombo, C. Shu, A. F. Adiyatullin, Z. Li, E. Mendez, B. Braverman, A. Kawasaki, D. Akamatsu, Y. Xiao, and V. Vuletić, Entanglement-enhanced optical atomic clock, arXiv:2006.07501.
[17] M. W. Itano, J. C. Bergquist, J. J. Bollinger, J. M. Gilligan, D. J. Heinzen, F. L. Moore, M. G. Reizen, and D. J. Wineland, Quantum projection noise: Population fluctuations in two-level systems, Phys. Rev. A **47**, 3554 (1993).
[18] V. Giovannetti, S. Lloyd, and L. Maccone, Quantum Metrology, Phys. Rev. Lett. **96**, 010401 (2006).
[19] L. Pezzè and A. Smerzi, Entanglement, Nonlinear Dynamics, and the Heisenberg Limit, Phys. Rev. Lett. **102**, 100401 (2009).
[20] D. J. Wineland, J. J. Bollinger, W. M. Itano, F. L. Moore, and D. J. Heinzen, Spin squeezing and reduced quantum noise in spectroscopy, Phys. Rev. A **46**, R6797(R) (1992).
[21] D. J. Wineland, J. J. Bollinger, W. M. Itano, and D. J. Heinzen, Squeezed atomic states and projection noise in spectroscopy, Phys. Rev. A **50**, 67 (1994).
[22] M. Kitagawa and M. Ueda, Squeezed spin states, Phys. Rev. A **47**, 5138 (1993).
[23] J. Ma, X. Wang, C. P. Sun, and F. Nori, Quantum spin squeezing, Phys. Rep. **509**, 89 (2011).
[24] D. Meiser, J. Ye, and M. J. Holland, Spin squeezing in optical lattice clocks via lattice-based QND measurements, New J. Phys. **10**, 073014 (2008).
[25] L. I. R. Gil, R. Mukherjee, E. M. Bridge, M. P. A. Jones, and T. Pohl, Spin Squeezing in a Rydberg Lattice Clock, Phys. Rev. Lett. **112**, 103601 (2014).
[26] C. Gross, T. Zibold, E. Nicklas, J. Estève, and M. K. Oberthaler, Nonlinear atom interferometer surpasses classical precision limit, Nature (London) **464**, 1165 (2010).
[27] M. F. Riedel, P. Böhi, Y. Li, T. W. Hänsch, A. Sinatra, and P. Treutlein, Atom-chip-based generation of entanglement for quantum metrology, Nature (London) **464**, 1170 (2010).
[28] T. Berrada, S. van Frank, R. Bücker, T. Schumm, J.-F. Schaff, and J. Schmiedmayer, Integrated Mach-Zehnder interferometer for Bose-Einstein condensates, Nat. Commun. **4**, 2077 (2013).
[29] J. G. Bohnet, B. C. Sawyer, J. W. Britton, M. L. Wall, A. M. Rey, M. Foss-Feig, and J. J. Bollinger, Quantum spin dynamics and entanglement generation with hundreds of trapped ions, Science **352**, 1297 (2016).
[30] J. Appel, P. J. Windpassinger, D. Oblak, N. Hoff, U. B. Kjeargaard, and E. S. Polzik, Mesoscopic atomic entanglement for precision measurements beyond the standard quantum limit, Proc. Natl. Acad. Sci. U.S.A. **106**, 10960 (2009).

[31] M. H. Schleier-Smith, I. D. Leroux, and V. Vuletić, States of an Ensemble of Two-Level Atoms with Reduced Quantum Uncertainty, Phys. Rev. Lett. **104**, 073604 (2010).

[32] J. G. Bohnet, K. C. Cox, M. A. Norcia, J. M. Weiner, Z. Chen, and J. K. Thompson, Reduced spin measurement back-action for a phase sensitivity ten times beyond the standard quantum limit, Nat. Photonics **8**, 731 (2014).

[33] O. Hosten, N. J. Engelsen, R. Krishnakumar, and M. A. Kasevich, Measurement noise 100 times lower than the quantum-projection limit using entangled atoms, Nature (London) **529**, 505 (2016).

[34] A. Louchet-Chauvet, J. Appel, J. J. Renema, D. Oblak, N. Kjaergaard, and E. S. Polzik, Entanglement-assisted atomic clock beyond the projection noise limit, New J. Phys. **12**, 065032 (2010).

[35] I. D. Leroux, M. H. Schleier-Smith, and V. Vuletić, Orientation-Dependent Entanglement Lifetime in a Squeezed Atomic Clock, Phys. Rev. Lett. **104**, 250801 (2010).

[36] B. Braverman *et al.*, Near-Unitary Spin Squeezing in 171Yb, Phys. Rev. Lett. **122**, 223203 (2019).

[37] R. J. Sewell, M. Koschorreck, M. Napolitano, B. Dubost, N. Behbood, and M. W. Mitchell, Magnetic Sensitivity Beyond the Projection Noise Limit by Spin Squeezing, Phys. Rev. Lett. **109**, 253605 (2012).

[38] W. Muessel, H. Strobel, D. Linnemann, D. B. Hume, and M. K. Oberthaler, Scalable Spin Squeezing for Quantum-Enhanced Magnetometry with Bose-Einstein Condensates, Phys. Rev. Lett. **113**, 103004 (2014).

[39] C. F. Ockeloen, R. Schmied, M. F. Riedel, and P. Treutlein, Quantum Metrology with a Scanning Probe Atom Interferometer, Phys. Rev. Lett. **111**, 143001 (2013).

[40] L. Salvi, N. Poli, V. Vuletić, and G. M. Tino, Squeezing on Momentum States for Atom Interferometry, Phys. Rev. Lett. **120**, 033601 (2018).

[41] A. Andrè, A. S. Sørensen, and M. D. Lukin, Stability of Atomic Clocks Based on Entangled Atoms, Phys. Rev. Lett. **92**, 230801 (2004).

[42] N. Shiga and M. Takeuchi, Locking the local oscillator phase to the atomic phase via weak measurement, New J. Phys. **14**, 023034 (2012).

[43] J. Borregaard and A. S. Sørensen, Near-Heisenberg-Limited Atomic Clocks in the Presence of Decoherence, Phys. Rev. Lett. **111**, 090801 (2013).

[44] E. M. Kessler, P. Kómár, M. Bishof, L. Jiang, A. S. Sørensen, J. Ye, and M. D. Lukin, Heisenberg-Limited Atom Clocks Based on Entangled Qubits, Phys. Rev. Lett. **112**, 190403 (2014).

[45] M. Mullan and E. Knill, Optimizing passive quantum clocks, Phys. Rev. A **90**, 042310 (2014).

[46] K. Chabuda, I. D. Leroux, and R. Demkowicz-Dobrzański, The quantum Allan variance, New J. Phys. **18**, 083035 (2016).

[47] M. Schulte, C. Lisdat, P. O. Schmidt, U. Sterr, and K. Hammerer, Prospects and challenges for squeezing-enhanced optical atomic clocks, arXiv:1911.00882 [Nat. Commun. (to be published)].

[48] R. Kohlhaas, A. Bertoldi, E. Cantin, A. Aspect, A. Landragin, and P. Bouyer, Phase Locking a Clock Oscillator to a Coherent Atomic Ensemble, Phys. Rev. X **5**, 021011 (2015).

[49] G. Colangelo, F. M. Ciurana, L. C. Bianchet, R. J. Sewell, and M. W. Mitchell, Simultaneous tracking of spin angle and amplitude beyond classical limits, Nature (London) **543**, 525 (2017).

[50] K. Hammerer, A. S. Srensen, and E. S. Polzik, Quantum interface between light and atomic ensembles, Rev. Mod. Phys. **82**, 1041 (2010).

[51] F. Rihele, *Frequency Standards: Basics and Applications* (Wiley-VCH, Weinhein, 2004).

[52] Here, $\hat{\boldsymbol{J}} = (\hat{J}_x, \hat{J}_y, \hat{J}_z)$ is the collective spin of the atomic ensemble, where $\hat{J}_{\boldsymbol{n}} = \sum_{j=1}^{N} \hat{\sigma}_{\boldsymbol{n}}^{(j)}/2$ and $\hat{\sigma}_{\boldsymbol{n}}^{(j)}$ is a Pauli operator along a direction $\boldsymbol{n}$ for the jth qubit.

[53] See Supplemental Material at http://link.aps.org/supplemental/10.1103/PhysRevLett.125.210503 for details on numerical and analytical results and a discussion about the impact of the imperfect implementation of the phase feedback.

[54] We have numerically simulated the clock operations, including the $1/f$ LO noise. None of the approximations used to derive the analytical expressions is used in the numerics. For the results of Fig. 2, we consider $N_c = 2000$ Ramsey cycles and average the inverse Allan variance over 50 independent realizations. Temporal correlations of the LO noise are included in the numerics.

[55] An optimization of the hybrid coherent-squeezed protocol over the squeezing parameter and the number of particles in each state leads to $\sigma^2_{\nu,\mathrm{opt}} = 4/(\omega_0^2 T \tau N_t^2)$ for $\nu \gg 1$, see L. Pezzè and A. Smerzi, Quantum phase estimation algorithm with Gaussian spin states, arXiv:2010.04001.

[56] T. Monz *et al.*, 14-Qubit Entanglement: Creation and Coherence, Phys. Rev. Lett. **106**, 130506 (2011).

[57] A. Omran *et al.*, Generation and manipulation of Schrödinger cat states in Rydberg atom arrays, Science **365**, 570 (2019).

[58] E. Davis, G. Bentsen, and M. Schleier-Smith, Approaching the Heisenberg Limit without Single-Particle Detection, Phys. Rev. Lett. **116**, 053601 (2016).

[59] F. Fröwis, P. Sekatski, and W. Dür, Detecting Large Quantum Fisher Information with Finite Measurement Precision, Phys. Rev. Lett. **116**, 090801 (2016).

[60] T. Macrì, A. Smerzi, and L. Pezzè, Loschmidt echo for quantum metrology, Phys. Rev. A **94**, 010102 (2016).

[61] O. Hosten, R. Krishnakumar, N. J. Engelsen, and M. A. Kasevich, Quantum phase magnification, Science **352**, 1552 (2016).

[62] J. Borregaard and A. S. Sørensen, Efficient Atomic Clocks Operated with Several Atomic Ensembles, Phys. Rev. Lett. **111**, 090802 (2013).

[63] T. Rosenband and D. R. Leibrandt, Exponential scaling of clock stability with atom number, arXiv:1303.6357.

[64] D. B. Hume and D. R. Leibrandt, Probing beyond the laser coherence time in optical clock comparisons, Phys. Rev. A **93**, 032138 (2016).

[65] W. Li, S. Wu, A. Smerzi, and L. Pezzè, Improvement of atomic clock stability with joint interrogation of two atomic ensembles (to be published).

[66] I. D. Leroux, N. Scharnhorst, S. Hannig, J. Kramer, L. Pelzer, M. Stepanova, and P. O. Schmidt, On-line

estimation of local oscillator noise and optimisation of servo parameters in atomic clocks, Metrologia **54**, 307 (2017).

[67] J. R. McClean, J. Romero, R. Babbush, and A. Aspuru-Guzik, The theory of variational hybrid quantum-classical algorithms, New J. Phys. **18**, 023023 (2016).

[68] N. Moll *et al.*, Quantum optimization using variational algorithms on near-term quantum devices, Quantum Sci. Technol. **3**, 030503 (2018).

[69] A. Peruzzo, J. McClean, P. Shadbolt, M.-H. Yung, X.-Q. Zhou, P. J. Love, A. Aspuru-Guzik, and J. L. OBrien, A variational eigenvalue solver on a photonic quantum processor, Nat. Commun. **5**, 4213 (2014).

[70] C. Kokail, C. Maier, R. van Bijnen, T. Brydges, M. K. Joshi, P. Jurcevic, C. A. Muschik, P. Silvi, R. Blatt, C. F. Roos, and P. Zoller, Self-verifying variational quantum simulation of the lattice Schwinger model, Nature (London) **569**, 355 (2019).

[71] R. D. Gill and S. Massar, State estimation for large ensembles, Phys. Rev. A **61**, 042312 (2000).

[72] D. W. Berry and H. M. Wiseman, Optimal States and almost Optimal Adaptive Measurements for Quantum Interferometry, Phys. Rev. Lett. **85**, 5098 (2000).

[73] H. M. Wiseman and G. J. Milburn, *Quantum Measurement and Control* (Cambridge University Press, Cambridge, England, 2009).

[74] M. Hayashi, Comparison between the Cramer-Rao and the mini-max approaches in quantum channel estimation, Commun. Math. Phys. **304**, 689 (2011).

[75] M. Hayashi, S. Vinjanampathy, and L. C. Kwek, Resolving unattainable Cramer-Rao bounds for quantum sensors, J. Phys. B **52**, 015503 (2019).